A New Modified Logistic Distribution: Properties and Applications in Uncertainty Data Modeling

A. M. Mohamed Ibrahim*[1], Zahid Khan[2], Fuad S. Al-Duais[3, 4]

[1] Department of Business Administration, College of Sciences and the Human Sciences in Alaflaj, Prince Sattam Bin Abdulaziz University, Saudi Arabia
[2] Department of Mathematics, Hazara University Mansehra, Pakistan
[3] Mathematics Department, College of Humanities and Science in Al Aflaj, Prince Sattam Bin Abdulaziz University, Al-Kharj, Saudi Arabia
[4] Business Administration Department, Administrative Science College, Thamar University, Thamar, Yemen

Emails: am.ibrahim@psau.edu.sa; zahidkhan@hu.edu.pk; f.alduais@psau.edu.sa

Abstract

The logistic distribution is widely used to model various types of applied data. The modified logistic distribution under neutrosophic statistics is introduced in this work. The neutrosophic logistic distribution (NLD) and its engineering applications are mainly emphasized. An appealing characteristic of the suggested NLD is that it is useful to many widely utilized survival assessment metrics, including the reliability function, hazard function, and survival function. Applications of some mathematical and statistical properties of the suggested model are discussed. Numerical investigations on simulated data are used to validate the theoretical findings experimentally. From an application point of view, it is inferred that the proposed distribution fits data with imprecise, hazy, and fuzzy information better than the usual model. In addition, the maximum likelihood (ML) technique for the proposed model is discussed under the neutrosophic inference framework. Eventually, some illustrative examples related to system reliability are provided to clarify further the implementation of the neutrosophic probabilistic model in real-world problems.

Keywords: Imprecise data; fuzzy statistics; neutrosophic probability; simulation; maximum likelihood estimation; Reliability

1. Introduction

The logistic distribution is used to analyze discrete and continuous data in a variety of engineering applications [1]. The logistic distribution is considered an alternative to the normal distribution with the same scaling parameter value, and it is substantially closer to the t-distribution with nine degrees of freedom [2]. Aside from this resemblance, it has a wider tail than typical normal density and can thus accommodate extreme observations exceptionally well in real-world data modeling [3]. Logistic distribution is useful for censoring data issues because its cumulative distribution function has a more manageable closed expression [4]. Interestingly, the logistic distribution is also a limiting form of the mean of the smallest and largest sample observations obtained from an exponentially symmetric model [5]. A thorough discussion of the applications of logistic distribution in many domains can be found in [6]. In the literature, the number of papers appeared on distinct types of generalizations of the logistic model, notably by [7]–[9]. Other significant contributions relevant to the logistic model's goodness of fit, skewed form, and inference procedures are provided in [6], [10], [11].

DOI: https://doi.org/10.54216/IJNS.200203
Received: November 20, 2022 Accepted: January 17, 2023

These generalizations are predicated on the idea that concise values may represent observable data or distributional characteristics. However, the impressions of physical quantities may be vague, fuzzy, unclear, diffuse, or imprecise [12]-[14]. Such types of uncertainties are considered non-probabilistic. Fuzzy probability is an approach of probability theory that deals with an uncertainty that is both probabilistic and non-probabilistic [15]. Fuzzy logic has been applied when evaluating the effectiveness of statistical tests in the context of uncertainty [16]. When there is ambiguity in the observations or parameters, fuzzy-based statistical methods have been used for estimation purposes [17]. The fuzzy-based statistical tests are proven more efficient than tests developed under classical statistics for analyzing imprecise data [18]. The main disadvantage of fuzzy logic is that it cannot provide information on the measure of indeterminacy. To address this limitation, Smarandache proposed the neutrosophic logic as an extension of fuzzy logic [19]. This notion became the basis for the extensions of several mathematical and statistical approaches in algebra, numerical algorithms, calculus, probability and estimation [20]. Smarandache proposed the neutrosophic descriptive statistics because of its potential uses for neutrosophic data, and they proved it to be more informative than traditional statistics [21]-[23]. Various statistical models under the neutrosophic statistics have been generalized for situations when the sample size, parameters of data generating model face some degree of uncertainty in their values. Neutrosophic distributions have been investigated in many studies including but not limited to [24]-[28]. Neutrosophic distributional models are increasingly being developed as viable replacements for their classical counterparts because they are flexible in the analysis of both precise and imprecise data [29]-[30]. Despite the growing popularity of probabilistic models, the theoretical aspects of statistical distributions and their relevance to diverse types of real-world data still need to be investigated.

Several generalizations of the logistic distribution generalization have been developed in mentioned literature; however, the features of the logistic model for inaccurate data remain largely unexplored. In fact, there is no logistic model for analyzing the neutrosophic data. Thus, this study aims to extend the scope of the logistic model to analyze the vague data that common exit in engineering applications.

The rest of the paper is organized as follows: In Section 2, we discuss some preliminaries of the proposed model. In Section 3, the suggested distribution and other significant features of the proposed model are presented. In Section 4, some essential characteristics of the proposed model are provided. Section 5 describes how to simulate data and define the quantile function of the proposed distribution. In Section 6, we give details on estimating unknown parameters under an uncertain environment using neutrosophic reasoning. Section 7 presents a comparative analysis of the proposed model with its existing counterpart. Section 8 provides some illustrative examples of the proposed model. Findings and Conclusions are presented in Section 9.

2. Preliminaries

Let the random variable T follows the logistic model with location parameter μ and scale parameter ρ then the cumulative distribution function (CDF) is given by:

$$G(t) = \frac{1}{1+e^{-\left(\frac{t-\mu}{\rho}\right)}}\ ; -\infty < t < \infty \quad (1)$$

where $\rho > 0$ and $\mu \in \mathcal{R}$. The corresponding probability density function (PDF) of T can be obtained by differentiating (1) as:

$$g(t) = \frac{e^{-\left(\frac{t-\mu}{\rho}\right)}}{\rho\left(1+e^{-\left(\frac{t-\mu}{\rho}\right)}\right)^2}\ ; -\infty < t < \infty,\ -\infty < \mu < \infty,\ \rho > 0 \quad (2)$$

If $\mu = 0$ and $\rho = 1$, then (2) is known as standard logistic distribution, and its PDF is defined as:

$$g(t) = \frac{e^{-(t)}}{(1+e^{-t})^2}\ ; -\infty < t < \infty \quad (3)$$

This distribution is notably used in reliability analysis, survival studies, and demographic data. The standard logistic distribution is symmetric about zero and has a kurtosis of 4.2. It is heavier tails than the normal distribution and has a more peaked form. Because of these characteristics, the logistic

DOI: https://doi.org/10.54216/IJNS.200203

Received: November 20, 2022 Accepted: January 17, 2023

density is a popular choice for fitting symmetric non-normal datasets. The shapes of PDF and CDF for different choices of μ and ρ are provided in Figure 1.

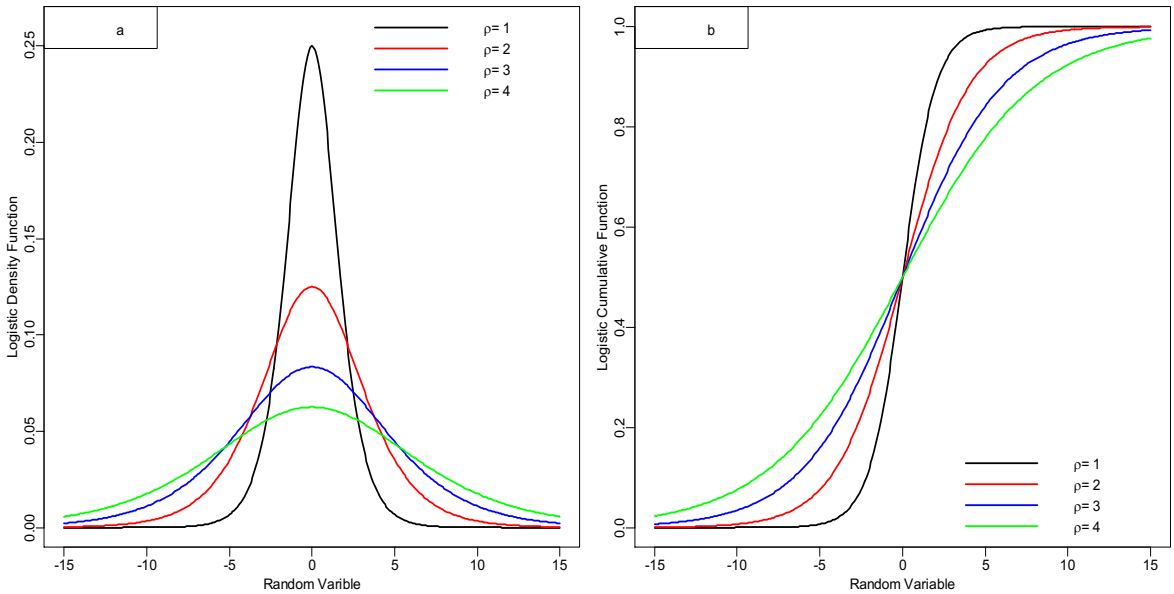

Figure 1: Basic graphs of the logistic distribution for different values of ρ when $\mu = 0$

Figure 1(a) shows that distribution is symmetric around location parameter μ and larger values of ρ result in more flatter density curves, whereas Figure 1(b) shows the probability of the CDF that varies from zero to one. This implies that the CDF must be zero when the PDF is at its smallest value. On the other end, CDF one infers that the random variable will be less than or equal to the maximum. Overall, CDF is a non-decreasing function.

Another closely related function of the logistic model is the survival function which can be deduced from (1) as:

$$S(t) = 1 - G(t) = \left(1 + e^{\left(\frac{t-\mu}{\rho}\right)}\right)^{-1} \quad (4)$$

Thus survival function provides the probability that random variable T is greater than the certain value t.

In the classical statistics framework, we have assumed that our distributional parameters are completely determined and have specific crisp values. This is a more realistic approach because, in many real data analyses, statistical models with uniquely defined parameters cannot adequately fit data, but we need to approximate the parameters of the data-generating process. This is one way of linking classical statistics to neutrosophic statistics. In neutrosophic statistics, data are based on incomplete, unsure, vague, or imprecise information instead of exactly known values of parameters.

3. Proposed Neutrosophic Distribution

This section concisely illustrates the proposed neutrosophic version of the logistic model. The following notions relate the proposed distribution to its practical applications in applied statistics. A random variable $\mathcal{T}$ is said to follow neutrosophic two parameters logistic model with the density function:

$$g_N(t) = \frac{e^{-\left(\frac{t-\mu_N}{\rho_N}\right)}}{\rho_N\left(1+e^{-\left(\frac{t-\mu_N}{\rho_N}\right)}\right)^2}; -\infty < t < \infty,\ -\infty < \mu_N < \infty,\ \rho_N > 0 \quad (5)$$

where $\mu_N = [\mu_l, \mu_u]$ and $\rho_N = [\rho_l, \rho_u]$ is the neutrosophic location and scale parameters, respectively of the NLD. Note that the proposed model differs from the existing structure of the classical logistic

DOI: https://doi.org/10.54216/IJNS.200203

Received: November 20, 2022 Accepted: January 17, 2023

distribution, where location and scale parameters are precisely determined. If we suppose that $\mu_l = \mu_u = \mu$ and $\rho_l = \rho_u = \rho$, then NLD converts to the classical form. Various values of the neutrosophic parameters result in different density curves, as given in Figure 2.

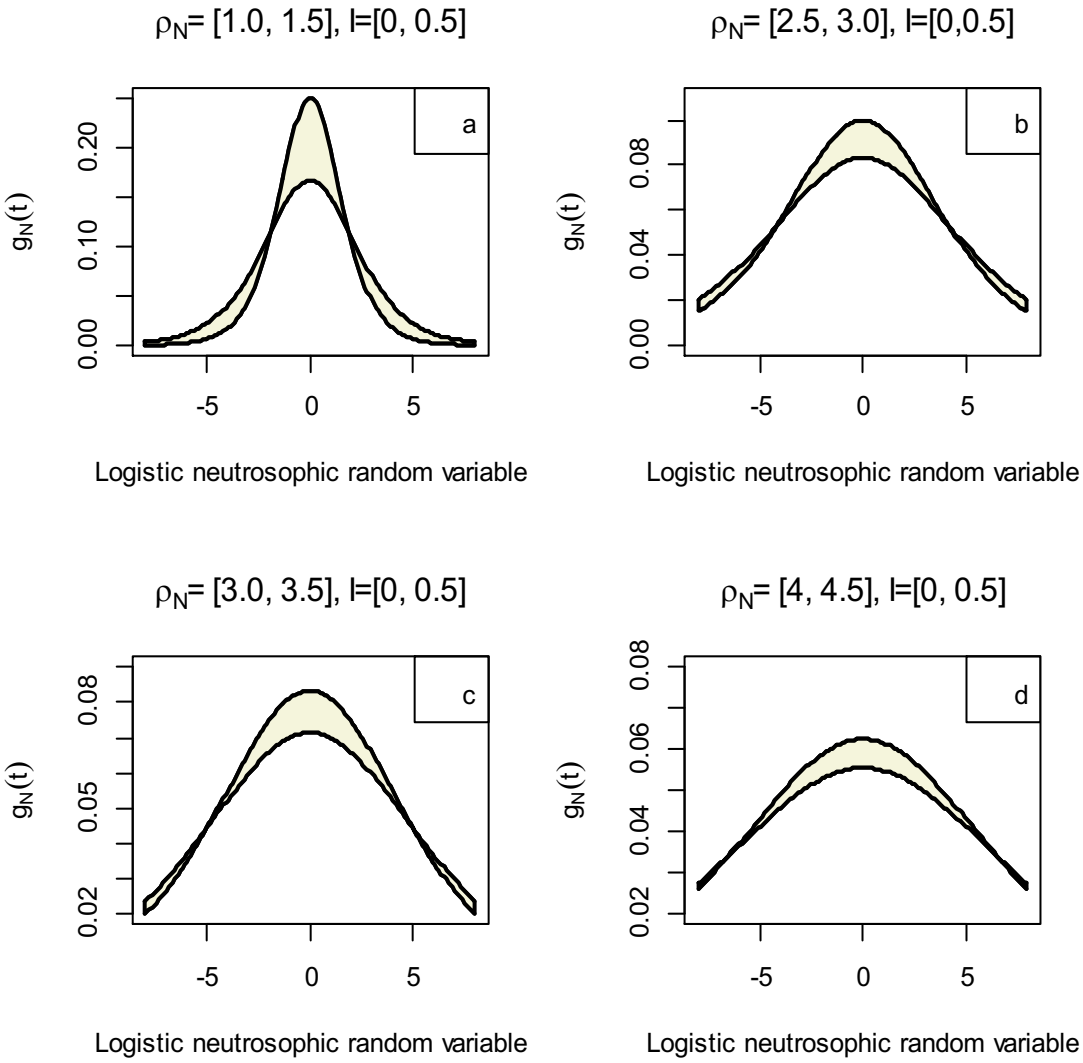

Figure 2: The density curves of the NLD with different values of ρ_N and $\mu_N = [0,\ 0]$

Figure 2 indicates that different indeterminate scale parameter values resulted in different sturdy curves of the NLD. Each density curve has been computed to varying values of indeterminacy factor I, associated with the scale parameter of the distribution. It is clear from Figure 1 that density curves are not well symmetric and distorted toward the right. The density curve is portrayed as a thick layer instead of a single curve in the neutrosophic framework. The layer width (shaded area) indicates an imprecision region, and the total area under the thick curve is one because of completeness. Another intriguing aspect of probability theory applications is the neutrosophic cumulative function (CF_N) of any density. The CF_N is a jointly coupled form of the (5) as:

$$G_N(t) = \frac{1}{1+e^{-\left(\frac{t-\mu_N}{\rho_N}\right)}} \qquad (6)$$

DOI: https://doi.org/10.54216/IJNS.200203
Received: November 20, 2022 Accepted: January 17, 2023

The CF_N function estimates the probability that a random variable will have a value smaller than the given value. Figure 3 indicates the CF_N curves for various interval values of the scale parameter of the proposed model.

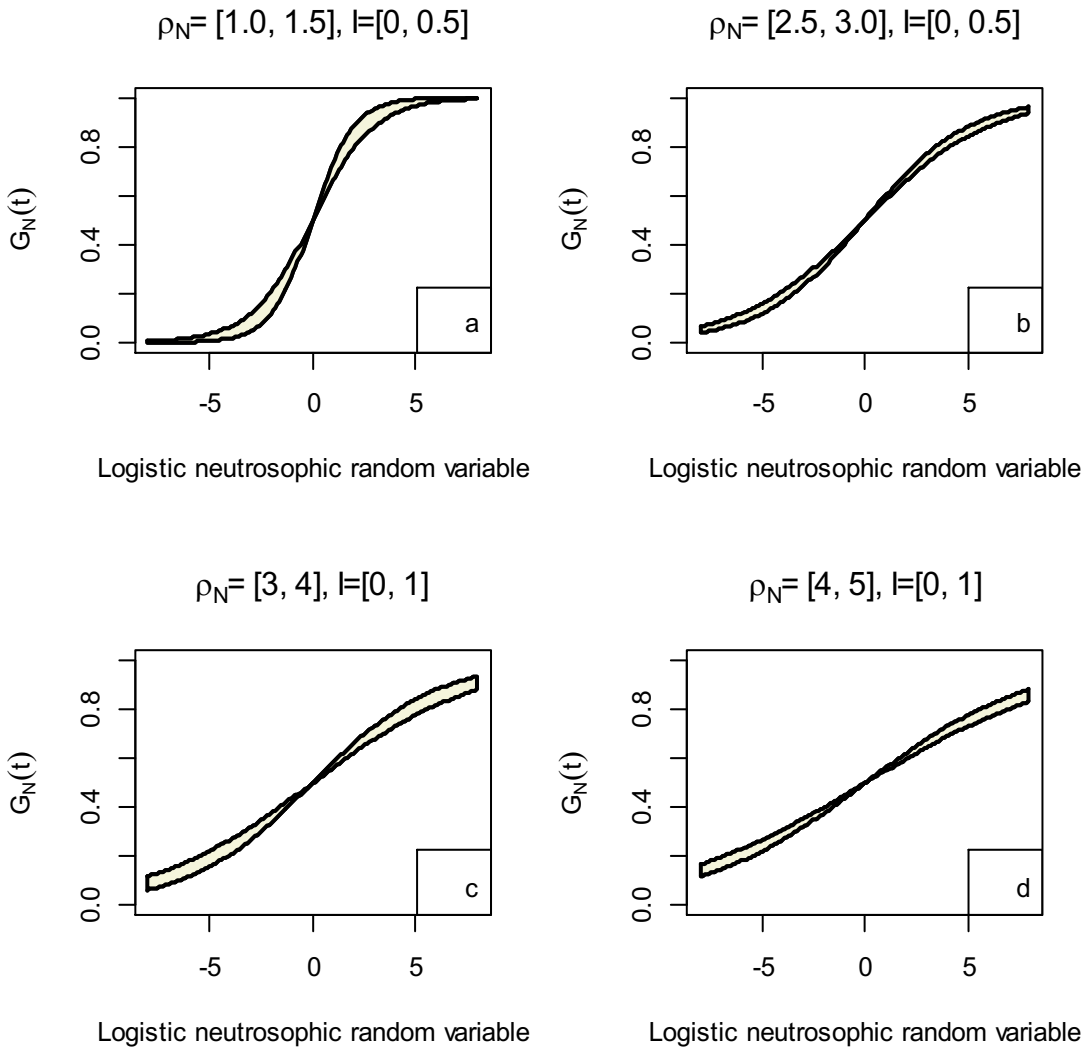

Figure 3: The cumulative curves of NLD at different values of ρ_N and $\mu_N = [0, 0]$

Figure 3 portrays the cumulative probabilities of the proposed model for various interval values of scale and fixed value of location parameters. In each panel of Figure 2, the CF_N is non-decreasing and varies between 0 and 1. The non-decreasing nature of the CF_N implies that the function cannot be negative and true for any distribution. The possibility that an individual will continue to live beyond a certain point in time is another important function in the probability theory. This function, known as the survival function or survival rate, represents the probability of an individual continuing to live beyond a certain point in time. The proposed model's survival function (SF_N) can be represented in the neutrosophic framework as follows:

$$S_N(t) = \frac{1}{1+e^{\left(\frac{t-\mu_N}{\rho_N}\right)}} \quad (7)$$

DOI: https://doi.org/10.54216/IJNS.200203
Received: November 20, 2022 Accepted: January 17, 2023

The graph that represents SF_N is known as a survival curve. Figure 4 portrays the survival curve for the proposed NLD. A steep curve in the graph can indicate a low survival rate or short survival period , as revealed in Figure 4b. A survival curve that remains steady or increases over time indicates a higher survival rate, as shown in Figure 4a.

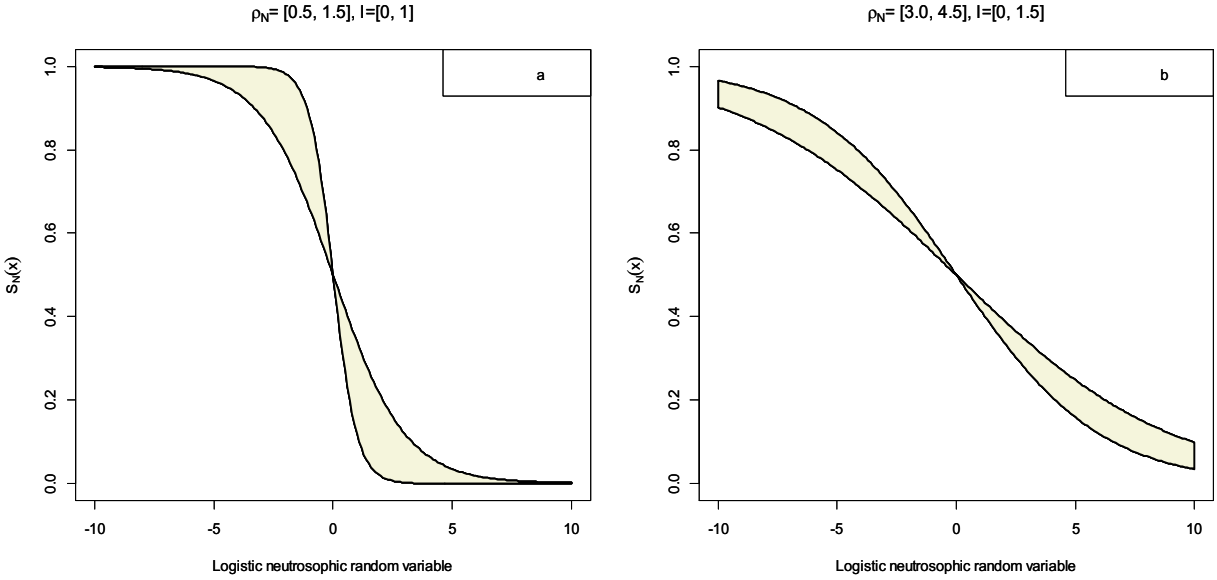

Figure 4: Survival function of the NLD for imprecise ρ_N and $\mu_N = [1,1]$

The hazard function (HF_N), also referred as the rate of imminent breakdown, is another essential function in reliability analysis. It is calculated by dividing the survival function by the density function, and its form for the proposed model is given as follows:

$$\hbar_N(t) = \frac{1}{\rho_N + \rho_N e^{\left(\frac{t-\mu_N}{\rho_N}\right)}} \tag{8}$$

The function HF_N represents the probability of failure for an individual or item over a specific period of time. The pattern of the hazard function may change over time and remains constant, decreases, increases or follows a more complex behavior.

4. Useful Properties

In this section, we have explored the theoretical foundations and examined some important distributional characteristics of the proposed NLD in the neutrosophic framework. For simplicity, the distribution characteristics that are parameterized as shown in (6) and (7) are provided below:

Theorem 1: If $\mathcal{T}$ follows the LD_N then $E(t) = \mu_N$

Proof: The mean of the NLD is defined below:

$$E(t) = \frac{1}{\rho_N}\int_{-\infty}^{\infty} \frac{e^{-\left(\frac{t-\mu_N}{\rho_N}\right)}}{\left[1+e^{-\left(\frac{t-\mu_N}{\rho_N}\right)}\right]^2} dt \tag{9}$$

By substituting $y_N = \frac{t-\mu_N}{\rho_N} = [y_l, y_u]$ in (9) yielded:

$$\rho_l \int_{-\infty}^{\infty} \frac{y_l e^{-y_l}}{(1+e^{-y_l})^2} dy_l + \mu_l \int_{-\infty}^{\infty} \frac{y_l e^{-y_l}}{(1+e^{-y_l})^2} dy_l = \mu_l$$

and

DOI: https://doi.org/10.54216/IJNS.200203
Received: November 20, 2022 Accepted: January 17, 2023

$$\rho_u \int_{-\infty}^{\infty} \frac{y_u e^{-y_u}}{(1+e^{-y_u})^2} dy_u + \mu_u \int_{-\infty}^{\infty} \frac{y_u e^{-y_u}}{(1+e^{-y_u})^2} dy_u = \mu_u$$

So it follows that:

$[\mu_l, \mu_u] = \mu_N$, hence proved.

Theorem 2: If $\mathcal{T}$ follow the NLD, then the mode is $g_N'(t) = \mu_N$

Proof: The mode of the NLD can be found as:

$$g_N'(t) = \frac{\frac{1}{\rho_N} e^{-\left(\frac{t-\mu_N}{\rho_N}\right)} \left(-\frac{1}{\rho_N}\right) \left[1+e^{-\left(\frac{t-\mu_N}{\rho_N}\right)}\right]^2 - e^{-\left(\frac{t-\mu_N}{\rho_N}\right)} 2\left[1+e^{-\left(\frac{t-\mu_N}{\rho_N}\right)}\right] e^{-\left(\frac{t-\mu_N}{\rho_N}\right)} \left(-\frac{1}{\rho_N}\right)}{\rho_N \left[1+e^{-\left(\frac{t-\mu_N}{\rho_N}\right)}\right]^4}$$

$$= \frac{\frac{1}{\rho_N{}^2} e^{-\left(\frac{t-\mu_N}{\rho_N}\right)} \left[1+e^{-\left(\frac{t-\mu_N}{\rho_N}\right)}\right]}{\left[1+e^{-\left(\frac{t-\mu_N}{\rho_N}\right)}\right]^4} \left\{\left[1+e^{-\left(\frac{t-\mu_N}{\rho_N}\right)}\right] - 2e^{-\left(\frac{t-\mu_N}{\rho_N}\right)}\right\} \quad (10)$$

Now $g_N'(t)$ equating to zero resulted:

$$\frac{\frac{1}{\rho_u{}^2} e^{-\left(\frac{t-\mu_u}{\rho_u}\right)} \left[1+e^{-\left(\frac{t-\mu_u}{\rho_u}\right)}\right]}{\left[1+e^{-\left(\frac{t-\mu_u}{\rho_u}\right)}\right]^4} \left\{\left[1+e^{-\left(\frac{t-\mu_u}{\rho_u}\right)}\right] - 2e^{-\left(\frac{t-\mu_u}{\rho_u}\right)}\right\} = 0$$

and

$$\frac{\frac{1}{\rho_l{}^2} e^{-\left(\frac{t-\mu_l}{\rho_l}\right)} \left[1+e^{-\left(\frac{t-\mu_l}{\rho_l}\right)}\right]}{\left[1+e^{-\left(\frac{t-\mu_l}{\rho_l}\right)}\right]^4} \left\{\left[1+e^{-\left(\frac{t-\mu_l}{\rho_l}\right)}\right] - 2e^{-\left(\frac{t-\mu_l}{\rho_l}\right)}\right\} = 0$$

Further simplification yielded the required result:

$\mu_N = [\mu_l, \mu_u]$

Theorem 3: If $\mathcal{T}$ follows the NLD, The variance of $\tilde{V}_N(t) = \frac{\rho_N^2 \pi^2}{3}$

Proof: Noting that variance of the NLD is:

$$\tilde{V}_N(t) = E(t^2) - [E(t)]^2 \quad (11)$$

The second raw moment is defined as:

$$E(t^2) = \frac{1}{\rho_N} \int_{-\infty}^{\infty} \mathcal{T}^2 \frac{e^{-\left(\frac{t-\mu_N}{\rho_N}\right)}}{\left[1+e^{-\left(\frac{t-\mu_N}{\rho_N}\right)}\right]^2} dt \quad (12)$$

$$= \left[\frac{1}{\rho_l} \int_{-\infty}^{\infty} t^2 \frac{e^{-\left(\frac{t-\mu_l}{\rho_l}\right)}}{\left\{1+e^{-\left(\frac{t-\mu_l}{\rho_l}\right)}\right\}^2} d\mathcal{T}, \frac{1}{\rho_u} \int_{-\infty}^{\infty} \mathcal{T}^2 \frac{e^{-\left(\frac{t-\mu_u}{\rho_u}\right)}}{\left\{1+e^{-\left(\frac{t-\mu_u}{\rho_u}\right)}\right\}^2} dt\right]$$

Further simplification can be rewritten as:

DOI: https://doi.org/10.54216/IJNS.200203
Received: November 20, 2022 Accepted: January 17, 2023

$$\left[\mu_l^2 + \frac{\rho_l^2\pi}{3}, \mu_u^2 + \frac{\rho_u^2\pi}{3}\right] = \mu_N^2 + \frac{\rho_N^2\pi^2}{3}$$

Equation (11) thus becomes

$\widetilde{V}_N(t) = \left[\frac{\rho_l^2\pi}{3}, \frac{\rho_u^2\pi}{3}\right] = \frac{\rho_N^2\pi^2}{3}$, hence proved.

Theorem 4: The skewness coefficient of the NLD is 0

Proof: The skewness coefficient for NLD can be derived as:

$$\hat{a}_3 = \frac{E(t) - g_N'(t)}{SD} \quad (13)$$

where $E(t) = \mu_N$, $g_N'(t) = \mu_N$, and SD stands for the standard deviation of the random variable $\mathcal{T}$.

Substituting in (14) yielded;

$\hat{a}_3 = 0$

Thus the coefficient of skewness is a crisp value.

Theorem 5: The kurtosis coefficient of the NLD is a constant quantity

Proof: Kurtosis coefficient for the NLD is defined as:

$$\hat{a}_4 = \frac{E(t^4)}{[\widetilde{V}_N(t)]^2} \quad (14)$$

where $E(t^4) = {}^{7\pi^4}/_{15}$ and $\widetilde{V}_N(t) = \frac{\pi^2}{3}$

Thus substituting in (11) yielded:

$\hat{a}_4 = {}^{21}/_{5}$

It follows that the excess of kurtosis of $\mathcal{T}$ is $\hat{a}_4 - 3 = \frac{6}{5}$

Hence the excess kurtosis is again a crisp quantity.

Similarly, some other useful notions of the proposed can be established in the neutrosophic framework.

5. Estimation Under Uncertainty

This section employs the commonly used maximum likelihood method to calculate the neutrosophic parameters of the proposed NLD. The maximum likelihood method involves evaluating the unknown parameters by determining the overall likelihood of all realizations in a dataset that are identically and independently distributed. After determining the likelihood of the NLD, the maximum point of the function is identified. These likelihood statistics are valuable from a statistical standpoint as they possess low variance and asymptotic unbiased characteristics. If $t_1, t_2, \ldots t_n$ are identical and independent observations that follow the suggested distribution defined in (1), the overall density is represented by:

$$\tau_N(\mu_N, \rho_N|\mathcal{T}) = \prod_{j=1}^{n} g_N(t_j) \quad (15)$$

(1) has the following probability function:

$$\tau_N(\mu_N, \rho_N|\mathcal{T}) = -n\ln(\rho_N) + \sum_{j=1}^{n}\left\{\frac{t_j-\mu_N}{-\rho_N}\right\} - 2\sum_{j=1}^{n}\ln\left(1+\exp\left\{\frac{t_j-\mu_N}{-\rho_N}\right\}\right) \quad (16)$$

In order to maximize τ_N, the gradient involving unknown values μ_N and ρ_N and is provided by:

$$\frac{\partial\tau_N}{\partial\mu_N} = \frac{n}{\rho_N} - \frac{2}{\rho_N}\sum_{j=1}^{n}\frac{1}{\left(1+\exp\left\{\frac{t_j-\mu_N}{\rho_N}\right\}\right)} = 0 \quad (17)$$

DOI: https://doi.org/10.54216/IJNS.200203
Received: November 20, 2022 Accepted: January 17, 2023

$$\frac{\partial \tau_N}{\partial \rho_N} = -\frac{n}{\rho_N} - \frac{1}{\rho_N}\sum_{j=1}^{n}\left(\frac{t_j-\mu_N}{\rho_N}\right)\frac{\left(1-\exp\left\{\frac{t_j-\mu_N}{\rho_N}\right\}\right)}{\left(1+\exp\left\{\frac{t_j-\mu_N}{\rho_N}\right\}\right)} = 0 \quad (18)$$

The solution of the simultaneous equations is the maximum likelihood estimators of μ_N and ρ_N.

$$\sum_{j=1}^{n}\left\{1+\exp\left[\frac{t-\mu_N}{\rho_N}\right]\right\}^{-1} = \frac{n}{2} \quad (19)$$

$$\sum_{j=1}^{n}\left(\frac{t_j-\mu_N}{\rho_N}\right)\frac{1-\exp\left[\frac{t_j-\mu_N}{\rho_N}\right]}{1+\exp\left[\frac{t_j-\mu_N}{\rho_N}\right]} = n \quad (20)$$

Note that μ_N and ρ_N will be interval values because of imprecise sample data. Additionally, we analyze the simulated dataset to demonstrate how the estimation procedure works in neutrosophic environment. For a given scale parameter value, 10,000 different samples from the NLD are generated with varying sizes at the fixed value of the location parameter. The behavior of ML estimator from unknown location parameter and scale parameter is also investigated in terms of neutrosophic root mean square error (RME_N). The values of ρ_N is taken as $[4, 6]$, whereas the value of the location parameter μ_N is fixed at [1, 1]. The RME_N is estimated according to the formula given below:

$$RME_N = \sqrt{\sum_{i=1}^{K}\frac{(\hat{\gamma}_i-\gamma_i)^2}{K}} \quad (21)$$

where γ_I and $\hat{\gamma}_i$ are respectively, actual and predicted values of the estimated parameter, and K is the total number of simulation runs. The R packages Metrics and EnvStats have been utilized to calculate the root mean square error values and estimate the model's parameters across various sample sizes. The estimated values of ρ_N at a fixed value of location parameter along with RME_N are reported in Table 1.

Table 1: Estimation and calculation of root mean square error using the neutrosophic ML approach

Sample size	$\hat{\rho}_N$	RME_N
15	[3.842, 5.763]	[0.870, 1.306]
30	[3.929, 5.893]	[0.611, 0.917]
60	[3.959, 5.939]	[0.430, 0.645]
90	[3.970, 5.955]	[0.351, 0.526]
120	[3.980, 5.971]	[0.306, 0.460]

Table 1 indicates that when the sample size increases, the value of the estimator tends to the benchmark value [2, 4], and RME_N drastically decreased. This trending behavior reveals that ML neutrosophic estimators efficiently perform with larger sample sizes. We can estimate and observe the performance of the location parameter λ_N but results are not presented here due to a similar trend.

6. Simulation Study

In this section, numerical investigations on simulated data are used to experimentally validate the theoretical results. We utilize a Monte Carlo approach to create random numbers that approximate the NLD distribution. The Monte Carlo method is a general term for any technique that involves random outcomes to solve a problem. The purpose of this investigation is to validate the theoretical findings outlined in Section 3 by generating random samples from the NLD and the Monte Carlo technique. The inverse CF_N approach has been considered as a most straightforward technique to simulate random numbers from the proposed model. This approach enables us to use a computer-built-in pseudo-random number generator for generating random numbers. The inverse CF_N of the proposed model is defined by:

DOI: https://doi.org/10.54216/IJNS.200203
Received: November 20, 2022 Accepted: January 17, 2023

$$G^{-1}(t) = \mu_N + \rho_N \ln\left(\frac{t_j}{1-t_j}\right) \quad (22)$$

where t_j randomly generated numbers from the uniform distribution and $G^{-1}(t)$ is desired percentile value of the proposed NLD. Suppose 10,000 random numbers are produced using the inverse CF_N approach from the suggested distribution with $\rho_N = [0.5,1]$ and $\mu_N = [3,3]$. It is worth mentioning that indeterminacy exists in the value of scale parameter i.e., $\rho_N = [2, 3.5]$ has an indeterminacy factor, $I = [0, 1.5]$. Analytical outcomes based on the analytical results given in Section 3 are calculated with baseline parameter values. Estimated values of different distribution properties, along with analytical findings and indeterminacy components, are presented in Table 2.

Table 2: Characteristics of the suggested distribution based on simulated data

Fundamental Characteristics	Analytical Results	Simulated Results
Mean	[3.000, 3.000]	[2.948, 2.970]
Variance	[0.822, 3.289]	[0.817, 3.268]
Median	[3.000, 3.000]	[2.948, 2.954]
Kurtosis Coefficient	[4.177, 4.177]	[4.177, 4.177]
Skewness Coefficient	[0.006, 0.006]	[0.006, 0.006]

Table 2 shows the summary statistics of the NLD for specified parameter values. The descriptive summary of the data generated by the suggested distribution is given in intervals due to the uncertainties in the defined parameters. However, some of the statistical characteristics in Table 2 have the same upper and lower bounds, indicating no uncertainty or definite values. As a result, the proposed model's foundation is validated by the strong agreement between the simulated and analytical results..

7. Comparative Study

In this section, the NLD has been compared with the classical counterpart in terms of the few numerical descriptive statistics. To estimate the value of descriptive statistics, a Monte Carlo technique is applied to generate the random numbers, expected to follow NLD and classical model at the average value of neutrosophic parameters. For the execution of NLD, we assume that $n_N = [2, 4]$ and $[6, 8]$ while the existing classical model is evaluated at average sample size values, i.e., $n = 3$ and 7. It has been further assumed that $\mu_N = [4, 4]$ and $\rho_N = [1, 1]$ in the simulation of 10000 different random samples from the proposed model. Thus the indeterminacy factor has been considered in sample size rather than distributional parameters. The values of descriptive summary are shown in Table 3 and Table 4.

Table 3: Comparative analysis of the proposed distribution with the classical model at $n_N = [2, 4]$

Basic Properties	Proposed Model	Existing Model
Location parameter	[3.980, 3.987]	3.982
Scale parameter	[0.644, 0.842]	0.784
Mean	[3.980, 3.987]	3.982
Standard deviation	[1.407, 1.635]	1.566
Median	[3.980, 3.987]	3.982
Kurtosis Coefficient	[4.197, 4.197]	4.197
Skewness Coefficient	[0.000, 0.000]	0.000

DOI: https://doi.org/10.54216/IJNS.200203
Received: November 20, 2022 Accepted: January 17, 2023

Table 4: Comparative analysis of the proposed distribution with the classical model at $n_N = [6, 8]$

Basic Properties	Proposed Model	Existing Model
Location parameter	[3.988, 3.990]	3.989
Scale parameter	[0.894, 0.924]	0.911
Mean	[3.988, 3.990]	3.989
Standard deviation	[1.689, 1.725]	1.710
Median	[3.980, 3.987]	3.989
Kurtosis Coefficient	[4.197, 4.197]	4.197
Skewness Coefficient	[0.000, 0.000]	0.000

It can be observed from the results reported in Table 3 and Table 4 that the existing logistic model provides values within the indeterminacy intervals. It is also worth mentioning here that suggested NLD provides equivalent results to the existing model when upper and lower limits of indeterminacy intervals become the same. Furthermore, estimated results become more accurate and reliable at a larger sample size, as shown in Table 4. In a nutshell, it is inferred from the simulation study that the proposed model is more efficient, flexible, and informative to be applied in an uncertain environment.

8. Illustrative Examples

In this section, we will demonstrate the proposed distribution's use in two examples related to reliability data. These examples are intended to illustrate how the proposed distribution can be applied in practical situations involving the estimation of system reliability.

Reliability estimation examines how likely it is that a system will work properly. If a system is made up of different parts that may or may not independently work, the reliability of the system depends upon the reliability of its parts. For example, a computer has many systems, each of which may have thousands of different parts. These components can fail, causing individual system failure and eventually leading to the failure of the unified setup. The reliability of a component is generally defined as the probability that it will work for a specific time period. This theory also considers systems with individual parts connected in parallel, in series, or a combination of both, whose failure probabilities can be described using neutrosophic probabilities obtained from the proposed NLD.

Example 1: For a computer to operate properly, all three components must be functioning correctly: the processor, the bus, and the memory. If we suppose that failure records of these three components following the NLD with chances of the processor and the bus functioning are both [92%, 94%] while the probability of the memory functioning is [96%, 98%]. How can the system reliability based on these components be estimated?

Here reliability figures are given in intervals, indicating that the probability of a specific event is not known exactly. This can be seen as a combination of three components that are connected in a series. Since a series system only functions when all of its components are functioning, the reliability of a system that has three components connected in a series is determined by multiplying the reliability of each individual component. Using the estimated neutrosophic probability and the multiplicative law of probability, we can calculate the desired reliability as follows:

$$R_N = [0.92, 0.94] \times [0.92, 0.94] \times [0.96, 0.98] = [0.82, 0.84]$$

Despite each individual component having a reliability of 92% or higher, the overall reliability of the computer is lower than 85%. On the other hand, the system with a parallel framework has built-in redundancy. If some of the components fail, the system will still function because there are backup components.

Example 2: Let failure times of a computer hard drive follow the NLD with [1%, 5%] probability of failure. Two additional hard drives with reliabilities of [95%, 98%] and [94%, 96%] can be used as backups. If all three storage drives are worked independently, the probability that the stored information is retained is calculated by determining the probability that none of the three hard drives crash. In this system, the data is saved on three hard disks in parallel. If all three disks fail, the information will be lost. However, as long as at least one of the three hard drives remains functional,

DOI: https://doi.org/10.54216/IJNS.200203
Received: November 20, 2022 Accepted: January 17, 2023

the information will be saved. Therefore, the likelihood that the information is stored in this parallel system can be calculated as follows:

$$R_N = 1 - \{[0.01, 0.05] \times [0.02, 0.05] \times [0.04, 0.06]\} = 1 - [8 \times 10^{-6}, 15 \times 10^{-4}] \cong 99\%$$

In the same way, reliability using the combinations of parallel and series systems can be estimated in an uncertain environment.

9. Conclusions

This study presented a novel generalized logistic distribution structure with the capability of fitting neutrosophic data in engineering applications. The assumptions of perfectly stated model parameters and indeterminacies make it impossible to apply the traditional logistic model in several practical situations. The newly proposed NLD has logistic distribution as a sub-model and high potential for practitioners in real data analysis. Several common statistical characteristics have been widely investigated in the context of neutrosophic statistics. Moreover, we provide numerous useful functions of the proposed model in the domain of reliability analysis and portray it in useful graphs to highlight its difference from the existing form of the logistic model. Theoretical findings of NLD have been further validated using simulated data. The maximum likelihood estimation has been employed to find the neutrosophic parameters and to evaluate their performance across various sample sizes. Results from simulated data indicated that the neutrosophic estimators efficiently perform with a larger sample size. A comparative analysis revealed that the proposed model is highly efficient, flexible, and informative for real data analysis. Additionally, some real-world examples have been provided to illustrate the practical usefulness of the suggested distribution in domain of engineering statistics.

Acknowledgement: The authors extend their appreciation to Prince Sattam Bin Abdulaziz University for funding this research work through the project number (PSAU/2022/02/22324)

Conflicts of Interest: The authors declare no conflict of interest.

References

[1] Pycke, J. R., A new family of omega-square-type statistics with Bahadur local optimality for the location family of generalized logistic distributions. Stat. Probab. Lett., vol. 170, p. 108999, 2021.

[2] Kumar, C. S. & Manju, L., Gamma Generalized Logistic Distribution: Properties and Applications. J. Stat. Theory Appl., vol. 21, no. 3, pp. 155–174, 2022.

[3] Mestry, D. V., & Bhowmick, A. R., On estimating the parameters of generalized logistic model from census data: Drawback of classical approach and reliable inference using Bayesian framework. Ecol. Inform., vol. 62, p. 101249, 2021.

[4] Rasekhi, M., Saber, M. M., & Yousof, H. M., Bayesian and classical inference of reliability in multicomponent stress-strength under the generalized logistic model. Commun. Stat., vol. 50, no. 21, pp. 5114–5125, 2020.

[5] Nigm, E. M., Records from reversed generalized logistic distribution and associated inference. J. Appl. Math. Comput. 2008 281, vol. 28, no. 1, pp. 249–264, 2008.

[6] Surendran, S. Tota-Maharaj, K., Log logistic distribution to model water demand data. Procedia Eng., vol. 119, no. 1, pp. 798–802, 2015.

[7] Li, G., & Qin, J., Analysis of two-sample truncated data using generalized logistic models. J. Multivar. Anal., vol. 97, no. 3, pp. 675–697, 2006.

[8] Mehdi S. M., & Yousof, H. M., Bayesian and Classical Inference for Generalized Stress-strength Parameter under Generalized Logistic Distribution. Stat. Optim. Inf. Comput., vol. x, pp. 0–12, 2021.

[9] Mathai, A. M., & Provost, S. B., On q-logistic and related models. IEEE Trans. Reliab., vol. 55, no. 2, pp. 237–244, 2006.

[10] Seo, J. I., & Kang, S. B., Notes on the exponentiated half logistic distribution. Appl. Math. Model., vol. 39, no. 21, pp. 6491–6500, 2015.

DOI: https://doi.org/10.54216/IJNS.200203
Received: November 20, 2022 Accepted: January 17, 2023

[11] Sun, R., Liu, M., & Zhao, L., Research on logistics distribution path optimization based on PSO and IoT. Int. J. Wavelets Multiresolution Inf., vol. 17, no. 6, 2019.

[12] Yager, R. R., Decision making with fuzzy probability assessments, IEEE Trans. Fuzzy Syst., vol. 7, no. 4, pp. 462–467, 1999.

[13] Patro, S. K., & Smarandache, F., The neutrosophic statistical distribution, more problems, more solutions. Infinite Study, 2016.

[14] Li, E. L., & Zhong, Y.-M., Random variable with fuzzy probability. Appl. Math. Mech. 2003 244, vol. 24, no. 4, pp. 491–498, 2003.

[15] Zadeh, L. A., Fuzzy sets as a basis for a theory of possibility. Fuzzy Sets Syst., vol. 1, no. 1, pp. 3–28, 1978.

[16] Yu, G., Measures of uncertainty for a fuzzy probabilistic information system. Int. J. Gen. Syst., vol. 50, no. 5, pp. 580–618, 2021.

[17] Figueroa-Garcia, J. C., Varon-Gaviria, C. A., & Barbosa-Fontecha, J. L., Fuzzy random variable generation using α-cuts. IEEE Trans. Fuzzy Syst., vol. 29, no. 3, pp. 539–548, 2021.

[18] Smarandache, F., A unifying field in logics: neutrosophic logic. neutrosophy, neutrosophic set, neutrosophic probability. American Research Press, Rehoboth, 1999.

[19] Smarandache, F., Neutrosophical statistics. Sitech & Education publishing, 2014.

[20] Khan, Z., Gulistan, M., Chammam, W., Kadry, S., & Nam, Y., A new dispersion control chart for handling the neutrosophic data. IEEE Access, vol. 8, pp. 96006–96015, 2020.

[21] Aslam, M., Analyzing wind power data using analysis of means under neutrosophic statistics. Soft Comput., vol. 25, no. 10, pp. 7087–7093, 2021.

[22] Aslam, M., Arif, O. H., & Sherwani, R. A. K., New diagnosis test under the neutrosophic statistics: An application to diabetic patients. Biomed Res. Int., vol. 2020, 2020.

[23] Haq, M. A. U., Neutrosophic kumaraswamy distribution with engineering application. NSS, vol. 49, no.1, p.17, 2022.

[24] Khan, Z., Gulistan, M., Hashim, R., Yaqoob, N., & Chammam, W., Design of S-control chart for neutrosophic data: An application to manufacturing industry. J. Intell. Fuzzy Syst., vol. 38, no. 4, pp. 4743–4751, 2020.

[25] Khan, Z., Gulistan, M., Kausar, N. & Park, C., Neutrosophic rayleigh model with some basic characteristics and engineering applications. IEEE Access, vol. 9, pp. 71277–71283, 2021.

[26] Aslam, M., Khan, N., & Khan, M., Monitoring the variability in the process using neutrosophic statistical interval method. Symmetry, vol. 10, no. 11, p. 562, 2018.

[27] Duan, W.Q., Khan, Z., Gulistan, M. & Khurshid, A., Neutrosophic exponential distribution: modeling and applications for complex data analysis. Complexity, vol. 2021, pp. 1–8, 2021.

[28] Aslam. M., Analyzing wind power data using analysis of means under neutrosophic statistics. Soft Computing, vol. 25, no.10, p. 7087-7093, 2021.

[29] Zhang, X., Bo, C., Smarandache, F., & Park, C., New operations of totally dependent-neutrosophic sets and totally dependent-neutrosophic soft sets. Symmetry, vol.10, no.6, p. 187, 2018.

[30] Abdelfattah,. A. M., Skew-Type I generalized logistic distribution and its properties. Pak. J. Stat. Oper. Res., vol. 11, no.3, pp. 267-282, 2015.

DOI: https://doi.org/10.54216/IJNS.200203
Received: November 20, 2022 Accepted: January 17, 2023